



Filamentation and linewidth enhancement factor in InGaAs quantum dot lasers

P. M. Smowton, E. J. Pearce, H. C. Schneider, W. W. Chow, and M. Hopkinson

Citation: [Applied Physics Letters](#) **81**, 3251 (2002); doi: 10.1063/1.1516236

View online: <http://dx.doi.org/10.1063/1.1516236>

View Table of Contents: <http://scitation.aip.org/content/aip/journal/apl/81/17?ver=pdfcov>

Published by the [AIP Publishing](#)



Re-register for Table of Content Alerts

Create a profile.



Sign up today!



Filamentation and linewidth enhancement factor in InGaAs quantum dot lasers

P. M. Smowton^{a)} and E. J. Pearce

Department of Physics and Astronomy, Cardiff University, Cardiff CF24 3YB, United Kingdom

H. C. Schneider and W. W. Chow

Semiconductor Materials and Device Sciences Department, Sandia National Laboratories, Albuquerque, New Mexico 87185-0601

M. Hopkinson

EPSRC Central Facility for III-V Semiconductors, University of Sheffield, Sheffield S1 3JD, United Kingdom

(Received 24 April 2002; accepted 30 August 2002)

We report measurements of the near-field of broad-area lasers with quantum dot and quantum well active regions designed to emit at 1 μm . The quantum dot devices exhibit less filamentation than comparable quantum well devices, and exhibit a reduction in filamentation as the injection level is increased. This is consistent with a theory that includes the Coulomb coupling between dot and wetting-layer states on a microscopic level. The theory predicts a linewidth enhancement factor from -3 to 1, depending on carrier density and inhomogeneous broadening. © 2002 American Institute of Physics. [DOI: 10.1063/1.1516236]

It has been suggested that high power lasers with quantum dot active regions should show significant performance advantages over conventional quantum well devices,^{1,2} and recently a single facet power of 4 W cw was reported at 10 °C.³ One of the important quantum dot characteristics with regard to high power performance is that they can exhibit a very low linewidth enhancement factor,⁴ which may reduce or remove filamentation in broad stripe devices. Filamentation occurs due to self focusing of the optical mode in the semiconductor gain medium, which results in a reduced lateral dimension of the fundamental mode, thus encouraging simultaneous lasing in higher order modes or filaments. It is primarily this effect that prevents simple scaling of the fundamental mode output power by increasing stripe width as is required for high output power devices.

In this work we have experimentally examined the degree of filamentation exhibited in broad area lasers with InGaAs quantum dot active regions emitting in the 1000 nm band, and have compared the results both with those for quantum well devices operating at the same wavelength and with theoretical predictions. In a real quantum dot laser the linewidth enhancement factor is non-zero because of many-body interactions⁵ and inhomogeneous broadening.⁶ Using a screened Hartree–Fock model, we have calculated the effects of many-body interactions between the dots and the wetting layer on the complex susceptibility.⁵ From the susceptibility we find the possibility of negative linewidth enhancement factors for highly excited quantum dots, with sufficiently small dot size and shape fluctuations.⁷ Using the calculated quantum dot susceptibility in a wave-optical laser model, we obtain an increasing filament width with increasing excitation. This is in contrast to the case of a quantum well laser in which the linewidth enhancement factor is generally positive

and the filament width decreases with increasing injection level.

The quantum dot laser structures consist of seven layers of $\text{In}_{0.5}\text{Ga}_{0.5}\text{As}$ deposited within 10 nm of GaAs at a growth temperature of 500 °C. These GaAs layers are separated by 7 nm of $\text{Al}_{0.15}\text{Ga}_{0.85}\text{As}$. The total separation between the dot layers, of GaAs and $\text{Al}_{0.15}\text{Ga}_{0.85}\text{As}$, is sufficient to electronically decouple subsequent layers of dots. The rest of the waveguide core of the device, of total width ≈ 220 nm, is made up of $\text{Al}_{0.15}\text{Ga}_{0.85}\text{As}$. The structures are clad with 1.2- μm -wide, doped $\text{Al}_{0.60}\text{Ga}_{0.40}\text{As}$ layers. The quantum dot size and density are estimated from field-emission scanning electron microscopy measurements on an uncapped structure grown using similar conditions. A dot density of $(5 \pm 1) \times 10^{10} \text{ cm}^{-2}$ and a dot diameter of ~ 20 – 25 nm are deduced. Low temperature photoluminescence measurements made on these structures show a broadened spectrum of width (FWHM) 32 ± 1 meV.⁸ Such a spectrum is consistent with a Gaussian broadening of the dot energy states due to size and/or shape fluctuations characterized by a standard deviation of approximately 14 meV. The quantum well laser structures have a single 10-nm-wide compressively strained $\text{In}_{0.22}\text{Ga}_{0.78}\text{As}$ well in 160 nm of $\text{Al}_{0.15}\text{Ga}_{0.85}\text{As}$ waveguide core that is clad with 1.2- μm -wide, doped $\text{Al}_{0.60}\text{Ga}_{0.40}\text{As}$ layers. These two structures are designed to operate at the same wavelength. The structures are fabricated into 50- μm -wide oxide isolated stripe lasers of lengths between 320 and 2000 μm . Measurement of the modal gain spectra indicated that lasing was obtained on the quantum dot ground state for all the device lengths investigated here.⁸

To remove any complications due to thermally induced self focusing, which occurs on a longer time scale,⁹ the devices were operated pulsed with a pulse width of 300 ns and a duty cycle of 0.03%. The laser near field was measured using an infrared camera with intervening neutral density filters adjusted to ensure that the camera did not saturate. For

^{a)}Electronic mail: smowtonpm@cf.ac.uk

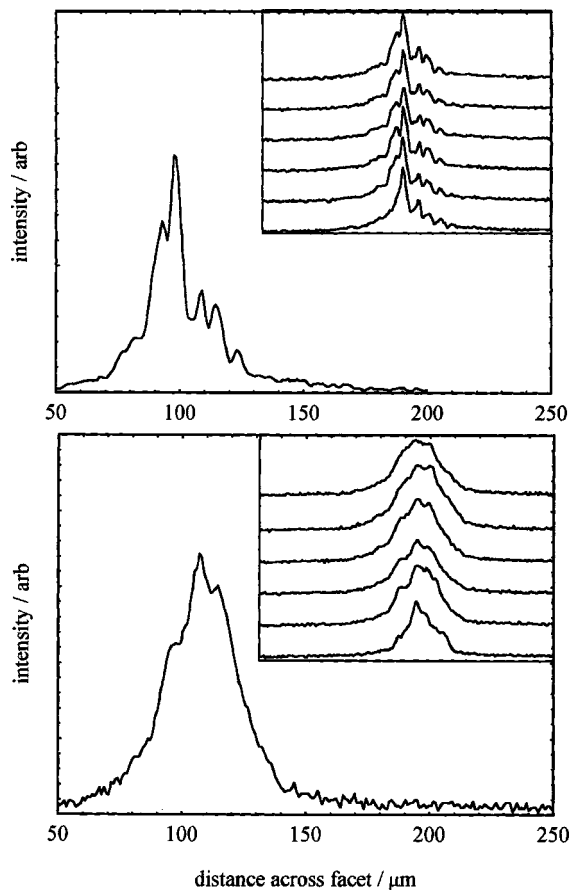


FIG. 1. Line scan of intensity through center of near field image for quantum well (above) and quantum dot (below) 50- μm -wide oxide isolated stripe lasers of length 550 μm and driven at $7\times$ threshold in the main part and between 5 and $12\times$ threshold in the insets.

each measurement the image was optimally focused and the near field recorded using image capture software. The near field appeared to be stable with time (times limited to greater than the 20 ms acquisition time of the camera system) and no changes were observed as the pulse length was varied between 100 and 1000 ns. The results were also unchanged when re-measured after an interval of 2 to 3 days. The near field was measured as a function of current and device length. An example of a line-scan of the intensity through the center of the near field image for a 550- μm -long quantum well device driven at seven times the threshold current injection level is given in the main part of the upper section of Fig. 1. The region exhibiting an intensity level above the background level is approximately the 50 μm width of the oxide isolated stripe. The uneven intensity distribution is typical of the results for the quantum well devices and reveals the presence of seven filaments across the 50 μm width. The inset shows further data taken between $5\times$ threshold and $12\times$ threshold offset on the y-axis for clarity. The threshold current of this device was 105 mA. An example, which is also typical, of a 550- μm -long quantum dot laser near field—also driven at $7\times$ threshold—is presented in the main part of the lower portion of Fig. 1. An uneven intensity distribution is apparent in the line scan; however, both the number of filaments and the depth of modulation of the intensity profile are reduced for the quantum dot samples. Again the inset shows further data taken between 5 and 12

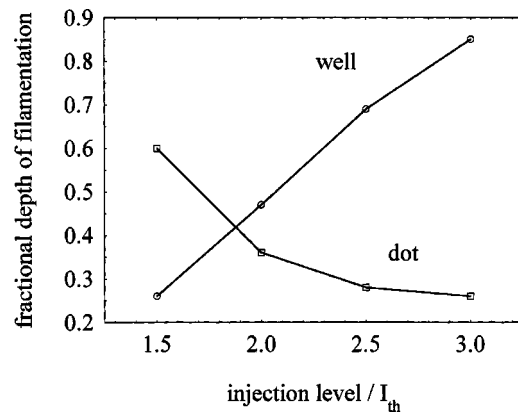


FIG. 2. Measured fractional depth of filamentation $(I_{\max} - I_{\min})/I_{\max}$ as a function of drive current relative to threshold for a typical quantum well (circles) and quantum dot (squares) laser.

\times threshold where the threshold current of the quantum dot device was 130 mA. We also observed that the depth of modulation of the intensity profile changed as a function of drive current, particularly at lower currents. An example of typical behavior is plotted in Fig. 2, where the fractional depth of filamentation is plotted as a function of injection level relative to threshold for a dot and well device. The fractional depth of filamentation is defined as $(I_{\max} - I_{\min})/I_{\max}$, where I_{\max} is the peak intensity and I_{\min} the valley intensity. A fractional depth of filamentation of 1 indicates complete modulation in light output from maximum to the background level across the near-field profile. All of the dot samples showed a reduction in depth of filamentation, or improvement, with increasing drive current, whereas the well samples showed the opposite behavior. We believe the improvement for the dot samples results from an increase in the filament width with drive current.

To model the behavior of our quantum dot lasers we used a microscopic theory⁵ to compute the complex susceptibility for a shallow quantum dot system for different carrier densities. In addition to changes in the gain (imaginary part of the susceptibility), we also obtain changes in the real part of the susceptibility (the carrier induced refractive index). These quantities also allow us to determine the linewidth enhancement factor,⁷ which is plotted in Fig. 3 as a function

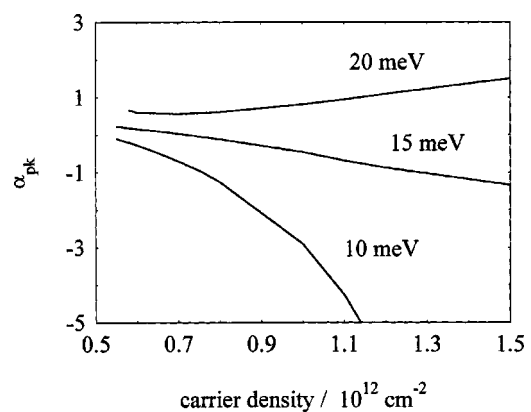


FIG. 3. Computed linewidth enhancement factor at gain peak vs carrier density for a model quantum dot and wetting-layer system for different degrees of inhomogeneous broadening. The dot density is $5\times 10^{10} \text{ cm}^{-2}$ and the material parameters are typical for InGaAs/AlGaAs systems.

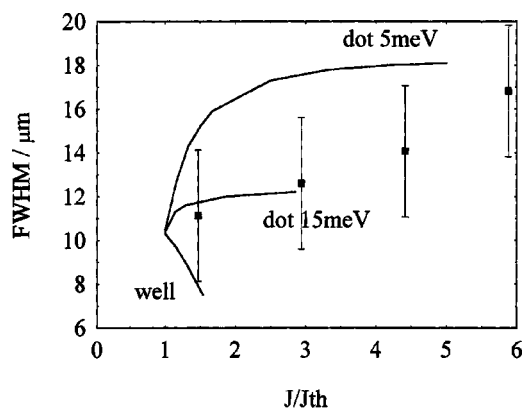


FIG. 4. Computed filament FWHM for a stripe device of length $500\ \mu\text{m}$ containing a quantum well (lower curve) and quantum dots with inhomogeneous broadening widths of 5 and 15 meV (upper and middle curves respectively) as a function of drive current relative to threshold. Values derived from the experimental data for $550\text{-}\mu\text{m}$ -long quantum dot devices are shown as points.

of carrier density, and for three different inhomogeneous broadening widths. For inhomogeneous broadening characterized by a standard deviation of 10 or 15 meV, we find that the linewidth enhancement factor can be negative, which indicates that the excitation dependence of the filamentation behavior of a quantum dot laser should be drastically different from that of a quantum well laser.

Using the computed susceptibility as an input to an existing wave optical laser model¹⁰ confirms the unusual filamentation behavior of quantum dot lasers. In Fig. 4, we show the computed FWHM of the filaments in the near field for quantum dot lasers using inhomogeneous broadenings of 5 and 15 meV, respectively, and for a comparable InGaAs quantum well laser. It is apparent that, for sufficiently small inhomogeneous broadening, the filament width increases with drive current for the quantum dot lasers, in agreement with our measurements, whereas in the quantum well laser case the filament width drastically decreases with excitation. We have also included experimentally determined filament widths in Fig. 4. These widths are extracted from the measured data by deconvolving the individual filaments within

each near field, and therefore exhibit appreciable variations as indicated by the error bars. The comparison shows that the experimental behavior is consistent with that predicted for a quantum dot laser with an inhomogeneous broadening of 15 meV. This degree of inhomogeneous broadening agrees with the broadening observed in low temperature photoluminescence measurements.

In summary, we have shown experimentally and theoretically that quantum dot lasers exhibit less filamentation than quantum well devices. The injection level dependence of the filament width is consistent with a many-body theory of an inhomogeneously broadened dot-wetting layer system. Based on our calculations, we predict linewidth enhancement factors between -3 and 1 , depending on inhomogeneous broadening.

One of the authors (E.J.P.) is supported by the U.K. Engineering and Physical Sciences Research Council and receives a CASE award from Bookham Technology (formerly Marconi Optical Components). Sandia is a multiprogram laboratory operated by Sandia Corporation, a Lockheed Martin Company, for the United States Department of Energy under Contract No. DE-AC04-94AL85000.

¹F. Heinrichsdorff, C. Ribbat, M. Grundmann, and D. Bimberg, *Appl. Phys. Lett.* **76**, 556 (2000).

²A. E. Zhukov, A. R. Kovsh, S. S. Mikrin, N. A. Maleev, V. M. Ustinov, D. A. Livshits, I. S. Tarasov, D. A. Bedarev, M. V. Maximov, A. F. Tsatsul'nikov, I. P. Soshnikov, P. S. Kop'ev, Zh. I. Alferov, N. N. Ledentsov, and D. Bimberg, *Electron. Lett.* **35**, 1845 (1999).

³F. Klopff, J. P. Reithmaier, A. Forchel, P. Collet, M. Krakowski, and M. Calligaro, *Electron. Lett.* **37**, 353 (2001).

⁴T. C. Newell, D. J. Bossert, A. Stintz, B. Fuchs, K. J. Malloy, and L. F. Lester, *IEEE Photonics Technol. Lett.* **11**, 1527 (1999).

⁵H. C. Schneider, W. W. Chow, and S. W. Koch, *Phys. Rev. B* **64**, 115315 (2001).

⁶D. Bimberg, N. Kirstaedter, N. N. Ledentsov, Zh. I. Alferov, P. S. Kop'ev, and V. M. Ustinov, *IEEE J. Sel. Top. Quantum Electron.* **3**, 196 (1997).

⁷H. C. Schneider, W. W. Chow, and S. W. Koch, accepted for publication in *Phys. Rev. B* **66**, 041310 (2002).

⁸P. M. Snowton, E. Herrmann, Y. Ning, H. D. Summers, P. Blood, and M. Hopkinson, *Appl. Phys. Lett.* **78**, 2629 (2001).

⁹J. G. McInerney, P. O'Brien, P. Skovgaard, M. Mullane, J. Houlihan, E. O'Neill, J. V. Moloney, and R. A. Indik, *Proc. SPIE* **3944**, 376 (2000).

¹⁰W. W. Chow and D. Depatie, *IEEE J. Quantum Electron.* **24**, 1297 (1988).